PHYSICAL REVIEW B VOLUME 36, NUMBER 7 1 SEPTEMBER 1987

X-ray absorption measurements on high-T_c superconductors: Cu-valence and cation-bond-length effects

Y. Jeon, F. Lu, H. Jhans, S. A. Shaheen, G. Liang, and M. Croft
Physics Department, Rutgers University, Piscataway, New Jersey 08855-0849

P. H. Ansari
Seton Hall University, South Orange, New Jersey 07079

K. V. Ramanujachary, E. A. Hayri, S. M. Fine, S. Li, X. H. Feng, and M. Greenblatt
Department of Chemistry, Rutgers University, Piscataway, New Jersey 08855-0939

L. H. Greene and J. M. Tarascon
Bell Communications Research, Red Bank, New Jersey 07701-7020
(Received 9 June 1987)

We present the results of Cu and Y K-edge and rare-earth and Ba L-edge x-ray absorption measurements on a series of new quaternary high-T_c superconducting compounds $La_{2-x}Sr_xCuO_{4-y}$ and $RBa_2Cu_3O_7$ (R=Y, Er, and Ho). The Cu K-edge results are shown to reflect the Cu valence state in these materials. The other measurements are discussed in the context of binary rare-earth oxides and the quantitative influence of bond lengths on continuum resonances in such spectra.

The electronic and structural properties of the new high-temperature superconducting materials is of course of great current interest.[1-4] In this paper, we present results of x-ray absorption near-edge spectroscopy (XANES) performed on both the $La_{2-x}Sr_xCuO_{4-y}$ and $RBa_2Cu_3O_7$ (R=Y, Er, and Ho) superconductors. We will discuss the near-edge structure of elements on each of the sublattices (except oxygen) in these materials. The Cu K-edge measurements will focus on the spectral evolution with increasing Cu valence. The Ba and R L-edge measurements revealed anticipated K_2NiF_4 structure for the $La_{2-x}Sr_xCuO_{4-y}$ series and $YBa_2Cu_3O_7$ structure for the $RBa_2Cu_3O_7$ series. Traces ($\sim$5%) of some unknown phase(s) were also observed except for $YBa_2Cu_3O_7$. All of the materials discussed here exhibited superconducting transition temperatures characteristic of other similar materials reported in the literature.[2,5,6] The x-ray absorption measurements were performed in the transmission mode on fine powders supported on tape at the Cornell high-energy synchrotron source (CHESS). Simultaneous standards were run for absolute energy calibration of the edge energies.

We show in Fig. 1 the superimposed Cu K-edge spectra of Cu-metal, Cu_2O, CuO, $YBa_2Cu_3O_7$, and $La_{2-x}Sr_xCuO_{4-y}$ ($x\sim0.15$). These spectra were taken simultaneously with a Cu-metal standard so that the relative onset energies of the edges are calibrated with respect to each other. The initial rise at the absorption edge moves to higher binding energy in this sequence of compounds as expected with increasing Cu valence.[7,8] The empirical fact that the onset of the Cu K edge occurs at higher energies than the formally Cu^{2+} oxide compound (CuO) supports the idea that the Cu valence state in the superconducting compounds is greater than Cu^{2+}. This is in accordance with expectation. It should also be noted, however, that we have found little, if any, discernible change in the Cu K edge in the $La_{2-x}Sr_xCuO_{4-y}$ compounds with varying x. Thus the shift of the Cu K edge is apparently not too sensitive to the Cu valence state in the Cu^{2+} to Cu^{3+} range.

We would now like to focus on the structure Cu K near edge in these compounds. Following Grunes,[9] Bair and Goddard,[10] and Kosugi, Yokoyama, Asakura, and Kuroda[11] we associate the peak C [see Fig. 1(a)] with $1s\rightarrow 4p$ transitions and the preedge peak B with $1s\rightarrow 4p$ transitions in the presence of a d-electron shakedown. Two effects combine in this shakedown process. First, Cu $3d$ states are pulled below the Fermi energy (ε_F) when the $1s$ core hole is created and, second, an electron makes a transition into this $3d$ level, leaving behind a hole state shared by the ligand atoms which are coordinated with the Cu atom (O atom in this case).[9-11] The $1s\rightarrow 4d+d$ shakedown transition occurs at an energy Δ below the $1s\rightarrow 4p$ transition where Δ is the energy of the shaken down d level below the Fermi energy.

With these peak assignments in mind, we interpret the above-noted Cu K-edge changes with increasing Cu valence as being rooted in the disappearance of the $4p+d$ shakedown feature. The closing of the d-shakedown channel with increasing Cu valence is accompanied by a transfer of spectral intensity to the normal $1s\rightarrow 4p$ transition (peak C).[9] In order to illustrate this interpretation we have used an arctangent function to simulate the onset

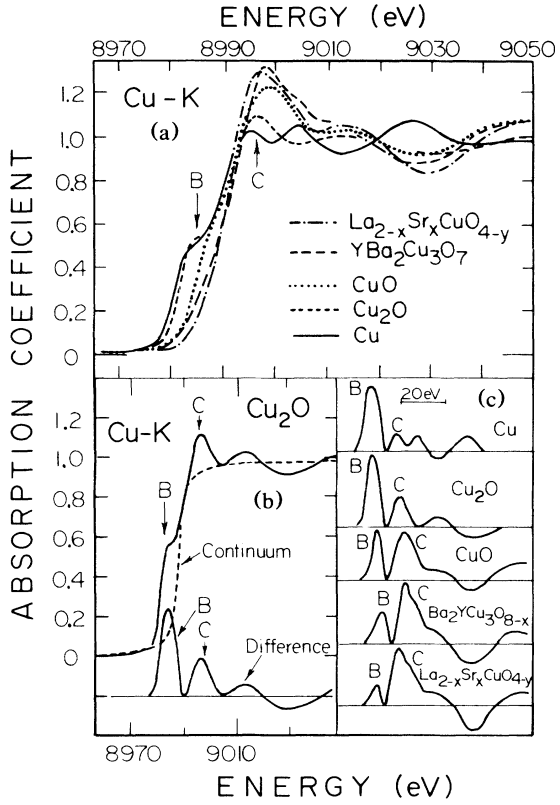

FIG. 1 (a) Cu K edges for elemental Cu, two Cu oxides, and two high-T_c superconducting compounds. (b) Illustration of the formation of a difference spectrum by subtracting an arctangent step function from the Cu_2O, Cu K spectrum. Here the arctangent function (labeled continuum) is used to approximate the $1s \rightarrow$ continuum transition. (c) Difference spectra for Cu compounds. Note the transfer of relative intensity from peak B to peak C with increasing Cu valence.

of $1s \rightarrow$ continuum transitions at the Cu K edge and have subtracted this contribution from each of the compound spectra to form "difference spectra." The virgin spectrum, arctangent function, and difference spectrum for Cu_2O are shown in Fig. 1(b). With the continuum onset approximately subtracted features, B and C, appear much more clearly in the compound difference spectra shown in Fig. 1(c). The difference spectra illustrate the increasing C feature intensity relative to the B feature intensity in the sequence Cu metal $\rightarrow Cu_2O \rightarrow$ CuO (i.e., with increasing Cu valence). In the superconducting compounds, the B feature (of d-shakedown origin) is even weaker than in the divalent standard CuO. This supports the notion that in the high-T_c superconducting compounds, the Cu valence is greater than 2+. The disappearance of the d-shakedown feature with increasing valence is presumably driven by the d^{10} state (which is shaken down) moving further above ε_F as the ground state is shifted beyond d^9 toward d^8. Thus, the peak assignments of Refs. 9–11 suggest a mechanism which offers some merit in understanding the Cu K-edge spectra of these compounds. Nevertheless, we feel that alternate mechanisms should also be considered. We prefer to emphasize here the empirical spectral evolution illustrated by our results in Fig. 1(c).

The rare-earth, Y, and Ba atoms in these superconducting materials are near-neighbor coordinated with oxygen; consequently, these materials are related to the R_2O_3 binary oxides. In Fig. 2, we show the rare-earth L_3 edges in both the binary and superconducting Er and Ho oxides. The dominant feature, labeled a, in these spectra is an atomic like $2p \rightarrow 5d$ transition and is commonly referred to as a "white line" (WL).[12] A second, weak feature (b) has been tentatively ascribed by previous authors to a many-body effect, and will not be discussed further here.[12] A third, strong feature (c) is usually referred to as a continuum or shape resonance and is associated with the existence of a shell or a cage of ligand atoms around the central absorbing atom.[13–16] The potential due to this ligand shell can cause a resonance in the continuum outgoing photoelectron spectrum for electronic $\mathbf{k}$ values (wavelengths) close to the ligand-shell geometrical resonance. This is analogous to the "almost-bound" particle in a finite-well-type problem. Rather than assume a specific model for the continuum resonance, we will start with the ansatz that its energy should be correlated with the radius (bond length) of its near-neighbor ligand shell. We will use the peak of the WL feature as the reference energy since it is clearly the best empirically defined energy in the near-edge spectra. That is, we will consider the energy differences ΔE_{ac} between the centers of peaks a and c.

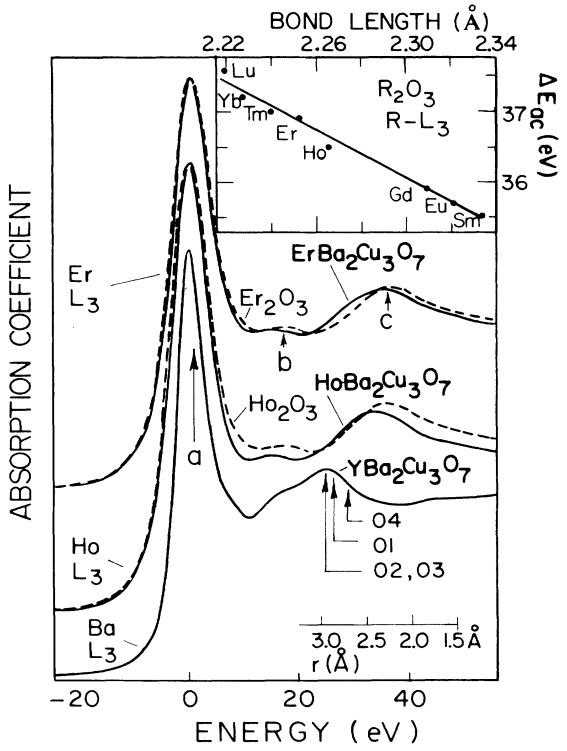

FIG. 2. RL_3 (R=Er and Ho) and Ba L_3 edges for $RBa_2Cu_3O_7$ and $YBa_2Cu_3O_7$ superconducting compounds. The length scale at the bottom of the figure is that empirically derived in the text for the continuum resonance feature. Inset: ΔE_{ac} vs R—O bond length in the cubic R_2O_3 compounds.

We have performed L_3-edge measurements on most of the heavy-rare-earth R_2O_3 oxides which occur in the cubic (distorted florite) structure. We plot in the inset of Fig. 2 the energy difference ΔE_{ac} versus the average R—O bond length in these materials (here the bond length is the equivalent florite bond length). There is a good linear correlation in these data and the solid fitted curve has the formula $\Delta E_{ac} = -mr + E_0$ with $m = 17.06$ eV/Å and $E_0 = +75.28$ eV or $r = r_0 - \Delta E_{ac}/m$ with $r_0 = 4.41$ Å. We have observed that the ΔE_{ac} value for the Er L_2 edge of Er_2O_3 falls very close to the corresponding L_3 edge ΔE_{ac} value, suggesting that this empirical bond-length correlation energy may be generalizable to the L_2 edge also.

In Fig. 2 we compare the R L_3 edges of $RBa_2Cu_3O_7$ to those of R_2O_3 where R = Er and Ho. In both cases, the quaternary oxide continuum resonance occurs at a smaller ΔE_{ac} value than in the binary oxide pointing to an expanded R—O bond length in the quaternary compound. If one extends the empirical relation determined above ($r = r_0 - \Delta E_{ac}/m$) to these compounds, one finds the bond-length (r) predictions shown in Table I. For comparison, we also show in Table I the observed Y—O bond length for the isostructural $YBa_2Cu_3O_7$ compound. The agreement suggests that our binary oxide ΔE_{ac}-r relation can reasonably be extended to these quaternary oxides.

Since the atomic $5d$ final states of the Ba L_3 edge are the same as at the rare-earth L_3 edges it makes sense to attempt to extend the above discussion to the Ba sites. We show in Fig. 2 (bottom) the Ba L_3 edge in the compound $YBa_2Cu_3O_7$. Relative to the R L_3 cases, the Ba L_3 continuum resonance is strongly shifted to smaller ΔE_{ac} values and shows a pronounced low-energy shoulder. The smaller ΔE_{ac} value is consistent with the observation that the Ba—O bond length is substantially expanded compared to the R—O (R = Er, Ho, or Y) bond length in this structure. Using our empirical relation ($r = 4.41 - \Delta E_{ac}/17.06$) we have placed a bond-length scale near the Ba L_3 spectrum. It should be noted that extrapolation of this empirical relation determined for the R_2O_3(R = heavy rare earth) compounds to the Ba site in the quaternary oxide can serve only a first approximation to be tested or improved upon. The arrows under the Ba L_3 spectrum indicate the known distribution of Ba—O bond lengths in $YBa_2Cu_3O_7$. As can be seen, the barium-oxygen bond lengths [O(1)-O(4)] do fall in the range of part of the Ba L_3 continuum resonance feature.

The reader should note that there is a distinct shoulder on the low-energy side of the continuum resonance in the Ba L_3 spectrum (see Fig. 2). Extrapolation of our energy versus neighbor distance scale would suggest that this shoulder may be caused by neighboring shells with clear "lines of sight" to the Ba sites at distances greater than 3.2 Å. Indeed, there are eight such Cu neighbors within 3.3–3.5 Å of the Ba and there are five Ba and one Y neighbors within 3.7–4.4 Å of the Ba. We, therefore, tentatively associate the spectral intensity in this energy range with these Ba, Y, and Cu neighboring shells.

Core s-state to above-ε_F p-state transitions are involved in the Er and Ba L_1-edge, and Y K-edge results shown in Fig. 3. As before, a prominent continuum resonance feature is present in all of the oxide spectra. By comparison, the relatively featureless Y metal K edge dramatically underscores the oxide continuum feature. The shift of the Er L_1 continuum feature closer to the edge on going from Er_2O_3 to $ErBa_2Cu_3O_7$ again reflects the bond-length expansion found above. The comparable energies (relative to the WL at the edge) of the Er L_1 and Y-K resonance features reflects the similar Er—O and Y—O bond lengths in the closely related Er and Y quaternary oxides. Finally, the Ba L_1 edge continuum resonance (in analogy to the L_3 results) shows more structure and a lower relative binding energy than in the above two Er and Y cases. This again supports the expanded nature of the Ba site and perhaps the enhanced contribution of more distant shells. A more quantitative analysis of the continuum resonance coupling to bond length in these materials is not possible at present, due to both the lack of other oxide L_1 and K-edge results and to the stronger more varied structure of the WL feature at these edges.

The strength and structure in the WL feature in these

TABLE I. Bond-length predictions.

	ΔE_{ac} (eV)	Predicted r (Å)
$ErBa_2Cu_3O_7$	L_3 35.2	2.35
	L_2 34.5	2.39
$HoBa_2Cu_3O_7$	L_3 34.5	2.39
$YBa_2Cu_3O_7$		$r_{obs} = 2.39$ Å[a]

[a]Reference 17.

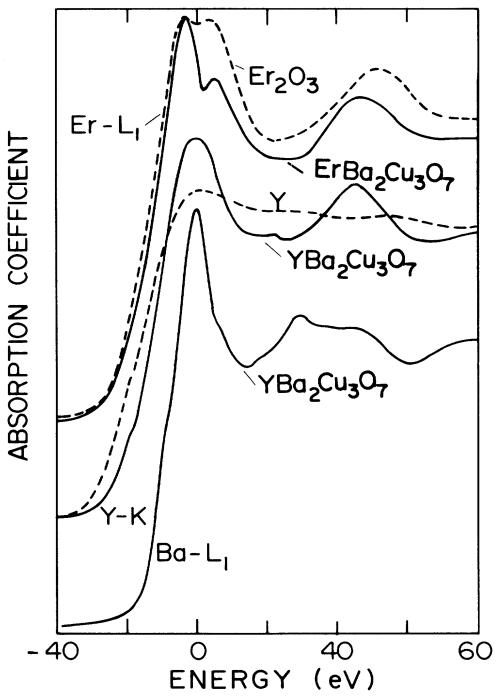

FIG. 3. The Er and Ba L_1 edges and Y K edge for selected superconducting compounds and standards.

oxide L_1 and K-edge spectra also deserve comment. The strength of these WL features indicates the presence of rather localized p states (i.e., Er $5p$, Ba $5p$, and Y $4p$) above ε_F in these materials. The localization of these states is emphasized by comparison of the strong oxide WL relative to the comparatively featureless Y metal K edge. Here the Y-metal $5p$ states are presumably strongly hybridized and itinerant. Finally, we note the bimodel structure of the WL at Er L_1 edges in Fig. 3 and the distinct pre-WL shoulder at the Ba L_1 edge in the same feature. A better basic and empirical understanding of these near-edge WL features is needed before detailed conclusions can be drawn.

In summary, our results suggest that x-ray absorption spectroscopy can potentially play several roles in helping to understand these interesting new classes of materials. Moreover, it also appears that these materials can provide a very useful proving ground for extending the utility of x-ray absorption near-edge spectroscopy.

This work was supported by State of New Jersey Commission on Science and Technology Grant No. 86-240040-13 and No. 87-240090-13, and Department of Energy Grant No. DE-F605-84-ER45081.

[1]J. G. Bednorz and K. A. Müller, Z. Phys. B **64**, 189 (1986).
[2]R. J. Cava, B. Batlogg, R. B. van Dover, and E. A. Rietman, Phys. Rev. Lett. **58**, 408 (1987).
[3]M. K. Wu, J. R. Ashburn, C. J. Torng, P. H. Hor, R. L. Meng, L. Gao, Z. J. Huang, Y. Q. Wang, and C. W. Chu, Phys. Rev. Lett. **58**, 908 (1987).
[4]J. M. Tarascon, L. H. Greene, W. R. McKinnon, G. W. Hull, and T. H. Geballe, Science **235**, 1373 (1987).
[5]R. J. Cava, B. Batlogg, R. B. van Dover, D. W. Murphy, S. Sunshine, T. Siegrist, J. P. Remeika, E. A. Rietman, S. Zahurak, and G. P. Espinosa, Phys. Rev. Lett. **58**, 1676 (1987).
[6]J. M. Tarascon, W. R. McKinnon, L. H. Greene, G. W. Hull, and E. M. Vogel, Phys. Rev. B **36**, 226 (1987).
[7]A. Nigam and M. Gupta, J. Phys. F **4**, 1084 (1974).
[8]O. Aggarwal and N. Saxena, Phys. Status Solidi (b) **122**, 669 (1984).
[9]L. A. Grunes, Phys. Rev. B **27**, 2111 (1983).
[10]R. Bair and W. Goddard III, Phys. Rev. B **22**, 2767 (1980).
[11]N. Kosugi, T. Yokoyama, K. Asakura, and H. Kuroda, Chem. Phys. **91**, 249 (1984).
[12]F. Jutzler, K. Hodgson, D. Misemer, and S. Doniach, Chem. Phys. Lett. **92**, 626 (1982).
[13]C. Natoli, in *EXAFS and Near Edge Structure III,* edited by K. O. Hodgson, B. Hedman, and J. E. Penner-Hahn (Springer-Verlag, New York, 1984), p. 38.
[14]A. Hitchcock, F. Sette, and J. Stöhr, in Ref. 13, p. 43.
[15]F. Settle, J. Stöhr, in Ref. 13, p. 250.
[16]J. Haase, Appl. Phys. A **38**, 181 (1985).
[17]M. Beno, L. Soderholm, D. Capone II, D. Hinks, J. Jorgensen, I. Schuller, C. Segre, K. Zhang, and J. Grace, Appl. Phys. Lett. **51**, 57 (1987).